Tetrahedron 67 (2011) 1011–1018

Contents lists available at ScienceDirect

Tetrahedron

journal homepage: www.elsevier.com/locate/tet

Acanthifoliosides, minor steroidal saponins from the Caribbean sponge *Pandaros acanthifolium*

Erik L. Regalado [a,*], Carlos Jiménez-Romero [b], Gregory Genta-Jouve [c], Deniz Tasdemir [d], Philippe Amade [c], Clara Nogueiras [e], Olivier P. Thomas [c,*]

[a] Department of Chemistry, Center of Marine Bioproducts (CEBIMAR), Loma y 37 Alturas del Vedado, C.P. 10400 Havana, Cuba
[b] Department of Chemistry, University of Puerto Rico, P.O. Box 23346, U.P.R. Station, San Juan, PR 00931-3346, Puerto Rico
[c] University of Nice-Sophia Antipolis, Laboratoire de Chimie des Molécules Bioactives et des Arômes UMR 6001 CNRS, Institut de Chimie de Nice, Faculté des Sciences, Parc Valrose, 06108 Nice Cedex 2, France
[d] University of London, School of Pharmacy, Department of Pharmaceutical and Biological Chemistry, Center for Pharmacognosy and Phytotherapy, 29-39 Brunswick Square, London WC1N 1AX, United Kingdom
[e] Center of Natural Products, Faculty of Chemistry, University of Havana, San Lázaro y L, Havana, Cuba

ARTICLE INFO

Article history:
Received 6 September 2010
Received in revised form 27 November 2010
Accepted 30 November 2010
Available online 13 December 2010

Keywords:
Marine sponge
Steroidal saponin
Pandaros
NMR
Circular dichroism

ABSTRACT

Seven novel steroid glycosides, acanthifoliosides A–F (**1**–**6**), and the methyl ester of **6** (**7**), were isolated from the marine sponge *Pandaros acanthifolium* as minor components. Acanthifoliosides are characterized by a rare C-15 and C-16 oxidized D ring, which was previously found in saponins produced by starfishes. Very uncommon is the presence of additional sugar residues at C-15 or C-16. Their structures were determined on the basis of extensive spectroscopic analyses, including two-dimensional NMR and HRESIMS data. The absolute configurations of the aglycones were assigned by comparison between experimental and TDDFT calculated CD spectra of **1**, whereas the absolute configurations of the monosaccharide units were determined by chiral GC analyses of the acid methanolysates. Some of the acanthifoliosides exhibit moderate antiprotozoal activity but to a lesser extent than the most potent pandarosides.

1. Introduction

Marine biodiversity has been recognized as a prolific source of original secondary metabolites with potential applications in the pharmaceutical industry. Even if most of the terrestrial families of natural products have been found in the marine environment, steroidal saponins are much more scarcely found in marine organisms than in their terrestrial counterparts. These compounds are mainly recognized as chemotaxonomic markers of echinoderms.[1] In marine sponges, triterpenoid saponins were mostly found in the *Asteropus*,[2–4] *Melophlus*,[5,6] and *Erylus*[7–9] genera all belonging to the Astrophorida order.

During our first investigation of the little studied Caribbean marine sponge *Pandaros acanthifolium* (Poecilosclerida, Microcionidae), a large family of 19 steroidal saponins named pandarosides was discovered as major constituents of this sponge.[10,11] So far, the only reported compound from this sponge was the polyether acanthifolicin.[12] Pandarosides are steroidal saponins, characterized by a rare 2-hydroxycyclopentenone D ring and a glucuronic acid at C-3, some of them bearing additional unsaturations in the A and B cycles. Most of these compounds exhibited interesting antiprotozoal activity, the most active being pandaroside G and its methyl ester, which potently inhibited the growth of *Trypanosoma brucei rhodesiense* and *Leishmania donovani*. Because some minor compounds with distinct UV and MS spectra were detected in the HPLC-DAD-MS profiles of some fractions, we decided to go further into the characterization of the secondary metabolome of this sponge, with the hope to isolate additional saponin derivatives.

Herein, we report the isolation and structural elucidation of a novel family of seven steroidal glycosides named acanthifoliosides A–F (**1**–**6**) and the methyl ester of **6** (**7**) as minor constituents of the sponge *P. acanthifolium* (Fig. 1). Their structures were elucidated by spectroscopic studies, including 1D and 2D NMR experiments as well as HRESIMS analyses. All of them lack the cyclopentenone D ring characteristic of the previous pandarosides. In vitro inhibitory activities of the new metabolites were evaluated against a small panel of parasitic protozoa, i.e., *T. b. rhodesiense*, *Trypanosoma cruzi*, *L. donovani*, and *Plasmodium falciparum*.

2. Results and discussion

The CH_2Cl_2/MeOH (1:1) extract of the Caribbean marine sponge *P. acanthifolium* was fractionated by RP-C_{18} flash chromatography

* Corresponding authors. Tel.: +33 492 076 314; fax: +33 492 076 599; e-mail address: olivier.thomas@unice.fr (O.P. Thomas).

0040-4020/$ – see front matter © 2010 Elsevier Ltd. All rights reserved.
doi:10.1016/j.tet.2010.11.103

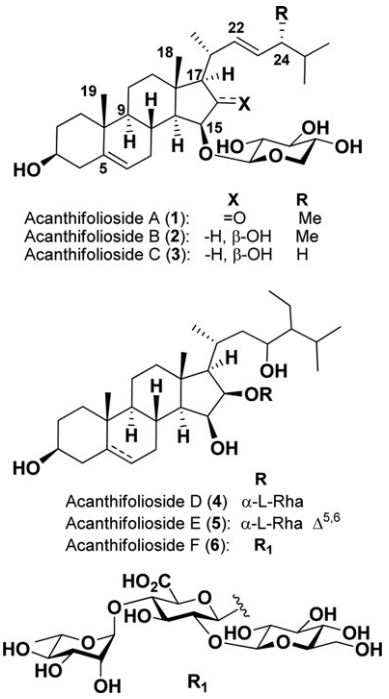

Fig. 1. Chemical structures of acanthifoliosides A–F (**1**–**6**).

and two complex polar fractions were further purified by successive semi-preparative RP-C_{18} HPLC and analytical C_6-phenyl HPLC to yield the seven new compounds **1**–**7** obtained as white amorphous solids.

The molecular formula of acanthifolioside A (**1**) was determined as $C_{33}H_{52}O_7$ by a pseudomolecular ion at m/z 583.3610 $[M+Na]^+$ in HRESIMS. The bands at 3490, 1688, and 1644 cm^{-1} in the IR spectrum suggested the presence of hydroxyl, carbonyl, and olefinic groups, respectively. The ^{13}C NMR spectrum of **1** confirmed the presence of 33 carbon signals, 28 of them corresponding to a steroid skeleton and five corresponding to a sugar portion according to the COSY and HSQC NMR spectra. The ^1H NMR spectrum of **1** evidenced characteristic steroid signals: two methyl groups placed on quaternary carbons at δ_H 1.06 (s, H_3-19) and 1.02 (s, H_3-18) and four methyl groups placed on tertiary carbons at δ_H 0.85 (d, J=6.8 Hz, H_3-26), 0.86 (d, J=6.8 Hz, H_3-27), 0.93 (d, J=6.8 Hz, H_3-24^1), and 1.13 (d, J=6.9 Hz, H_3-21) (Table 1).

These data were consistent with an ergostane skeleton. Analysis of the ^{13}C NMR spectrum of the aglycone part showed the occurrence of one olefinic quaternary carbon (δ_C 142.0), three olefinic methines (δ_C 135.3, 134.3, and 122.5), two secondary oxygenated carbons (δ_C 74.7 and 72.4), and one carbonyl (δ_C 218.9) (Table 2). The assignments of ^1H and ^{13}C signals of the tetracyclic ring system was established by a combination of COSY, HSQC, and HMBC data interpretation, starting from the HMBC correlations of the protons of the angular methyls Me-18 and Me-19. Long-range correlations from the proton signal at δ_H 1.06 (H_3-19) to the carbon resonances at

Table 1
^1H NMR data for acanthifoliosides A–F (**1**–**6**) at 500 MHz in CD_3OD. δ_H in ppm (mult., J in Hz)

No.	1	2	3	4	5	6
1β	1.89 (m)	1.89 (m)	1.87 (m)	1.73 (m)	1.88 (m)	1.74 (m)
1α	1.08 (m)	1.06 (m)	1.07 (m)	0.99 (m)	1.07 (m)	1.00 (m)
2α	1.81 (m)	1.79 (m)	1.78 (m)	1.77 (m)	1.77 (m)	1.53 (m)
2β	1.49 (m)	1.48 (m)	1.48 (m)	1.41 (m)	1.51 (m)	1.30 (m)
3	3.41 (tt, 10.9, 4.5)	3.39 (tt, 10.9, 4.9)	3.39 (tt, 10.9, 4.9)	3.51 (tt, 10.8, 4.9)	3.40 (tt, 10.8, 4.9)	3.77 (m)
4β	2.25 (m)	2.24 (m)	2.24 (m)	1.30 (m)	2.25 (m)	1.33 (m)
4α	2.22 (m)	2.21 (m)	2.21 (m)	1.53 (m)	2.22 (m)	1.71 (m)
5				1.14 (m)		1.13 (m)
6α	5.36 (br d, 4.8)	5.35 (br d, 5.0)	5.34 (br d, 4.8)	1.38 (m)	5.38 (br d, 4.8)	1.38 (m)
6β				1.33 (m)		1.34 (m)
7β	2.37 (m)	2.61 (m)	2.61 (m)	2.10 (m)	2.34 (m)	2.10 (m)
7α	1.61 (m)	1.50 (m)	1.50 (m)	1.01 (m)	1.64 (m)	1.01 (m)
8	1.94 (m)	1.86 (m)	1.86 (m)	1.84 (m)	1.97 (m)	1.83 (m)
9	1.15 (m)	1.08 (m)	0.99 (m)	0.71 (m)	1.01 (m)	0.71 (m)
11α	1.56 (m)	1.49 (m)	1.48 (m)	1.49 (m)	1.47 (m)	1.51 (m)
11β	1.64 (m)	1.52 (m)	1.51 (m)	1.52 (m)	1.53 (m)	1.54 (m)
12α	2.00 (m)	1.97 (m)	1.97 (m)	1.99 (m)	2.01 (m)	2.00 (m)
12β	1.41 (m)	1.12 (m)	1.12 (m)	1.09 (m)	1.09 (m)	1.10 (m)
14	1.50 (m)	0.97 (m)	0.94 (m)	0.86 (m)	0.88 (m)	0.86 (m)
15	4.06 (d, 7.3)	4.24 (t, 6.5)	4.24 (t, 6.5)	4.18 (dd, 6.2, 5.8)	4.18 (t, 6.3)	4.18 (t, 6.2)
16		4.26 (t, 7.2)	4.26 (t, 7.2)	4.27 (dd, 8.0, 6.3)	4.29 (t, 7.2)	4.28 (t, 7.1)
17	2.02 (d, 5.5)	1.05 (m)	1.04 (m)	1.18 (m)	1.18 (t, 7.3)	1.17 (t, 7.1)
18	1.02 (s)	1.05 (s)	1.01 (s)	1.05 (s)	1.06 (s)	1.04 (s)
19	1.06 (s)	1.07 (s)	1.04 (s)	0.87 (s)	1.07 (s)	0.88 (s)
20	2.53 (q, 6.9)	2.60 (m)	2.61 (m)	2.28 (m)	2.28 (m)	2.28 (m)
21	1.13 (d, 6.9)	1.08 (d, 6.6)	1.08 (d, 6.6)	1.01 (d, 6.6)	1.04 (d, 6.4)	1.01 (d, 6.6)
22a	5.61 (dd, 15.4, 7.8)	5.59 (dd, 15.6, 8.0)	5.60 (dd, 15.5, 7.3)	1.79 (m)	1.80 (m)	1.79 (m)
22b				0.98 (m)	1.01 (m)	1.01 (m)
23	5.32 (dd, 15.4, 7.8)	5.39 (dd, 15.6, 8.0)	5.46 (dt, 15.5, 6.8)	3.90 (ddd, 10.8, 4.5, 1.9)	3.90 (ddd, 10.8, 4.5, 1.9)	3.90 (ddd, 10.8, 4.5, 1.9)
24a	1.88 (m)	1.88 (m)	1.90 (m)	1.02 (m)	1.01 (m)	1.08 (m)
24b			1.86 (m)			
24^{1}a	0.93 (d, 6.8)	0.95 (d, 6.6)		1.47 (m)	1.49 (m)	1.47 (m)
24^{1}b				1.37 (m)	1.39 (m)	1.39 (m)
24^2				0.97 (t, 7.1)	0.97 (t, 7.3)	0.96 (t, 7.1)
25	1.50 (m)	1.50 (m)	1.59 (m)	1.87 (m)	1.87 (m)	1.87 (m)
26/27	0.85 (d, 6.8)	0.87 (d, 6.6)	0.86 (d, 6.6)	0.90 (d, 6.8)	0.91 (d, 6.7)	0.90 (d, 6.8)
	0.86 (d, 6.8)	0.87 (d, 6.6)	0.89 (d, 6.6)	0.96 (d, 6.8)	0.96 (d, 6.7)	0.93 (d, 6.8)
1′	4.77 (d, 7.8)	4.28 (d, 7.8)	4.28 (d, 7.8)	4.77 (d, 3.2)	4.79 (d, 3.2)	4.58 (d, 7.5)
2′	3.09 (dd, 8.9, 7.8)	3.20 (t, 8.4)	3.20 (t, 8.2)	4.09 (t, 3.2)	4.10 (t, 3.2)	3.44 (m)
3′	3.31 (t, 9.0)	3.29 (t, 8.9)	3.29 (t, 9.1)	3.78 (dd, 7.8, 3.2)	3.78 (dd, 8.0, 3.2)	3.53 (m)

Table 1 (*continued*)

No.	1	2	3	4	5	6
4′	3.48 (m)	3.48 (m)	3.48 (dd, 9.1, 6.6)	3.45 (t, 8.1)	3.45 (t, 8.3)	3.58 (m)
5′a	3.85 (dd, 11.5, 5.5)	3.85 (dd, 11.5, 5.5)	3.84 (dd, 11.5, 5.5)	3.83 (tt, 8.7, 6.2)	3.84 (tt, 8.7, 6.4)	3.77 (m)
5′b	3.18 (t, 10.9)	3.15 (t, 10.7)	3.15 (t, 10.7)			
6′				1.30 (d, 6.6)	1.30 (d, 6.2)	
1″ (Glu)						4.59 (d, 7.3)
2″						3.24 (m)
3″						3.38 (m)
4″						3.33 (m)
5″						3.29 (m)
6″a						3.84 (m)
6″b						3.71 (m)
1‴ (Rha)						4.77 (d, 3.2)
2‴						4.10 (t, 3.2)
3‴						3.78 (m)
4‴						3.46 (m)
5‴						3.85 (m)
6‴						1.30 (d, 6.2)

Table 2
^{13}C NMR data for acanthifoliosides A–F (**1**–**6**) at 125 MHz in CD_3OD. δ_C in ppm

No.	1	2	3	4	5	6
1	38.4	38.6	38.6	38.2	38.5	38.2
2	32.3	32.3	32.3	32.2	32.5	30.4
3	72.4	72.5	72.5	71.9	72.5	80.4
4	43.0	43.0	43.0	38.9	43.0	35.5
5	142.0	141.7	141.7	46.4	142.1	46.2
6	122.5	122.9	122.9	29.9	122.5	29.9
7	31.8	31.7	31.7	32.1	32.2	32.5
8	27.7	28.7	28.7	32.5	28.7	32.5
9	51.7	51.9	51.9	56.1	51.8	56.0
10	37.9	37.8	37.8	36.8	37.8	36.9
11	21.7	21.6	21.6	22.0	22.0	22.0
12	40.5	42.2	42.2	42.7	42.3	42.7
13	43.7	43.4	43.4	44.0	43.7	44.0
14	56.8	60.2	60.2	60.2	60.5	60.2
15	74.7	79.0	79.0	71.2	71.2	71.4
16	218.9	74.6	74.5	86.2	86.1	86.2
17	69.0	63.8	63.6	63.9	63.9	64.0
18	17.9	16.0	15.9	16.5	16.2	16.5
19	19.7	19.8	19.7	12.7	19.8	12.8
20	35.6	34.2	34.7	28.0	28.0	28.0
21	21.6	20.6	20.6	18.2	18.2	18.2
22	135.3	137.1	139.2	43.6	43.5	43.7
23	134.3	133.5	128.0	70.0	69.9	70.3
24	44.4	44.5	43.4	54.0	54.0	54.0
24^1	18.1	18.1		20.5	20.4	20.5
24^2				15.1	15.1	15.2
25	34.5	34.4	29.8	29.6	29.6	29.6
26/27	20.3	20.2	22.7	20.1	20.1	20.1
	21.5	20.4	22.8	21.5	21.5	21.5
1′	103.5	105.4	105.3	105.1	105.1	105.2
2′	75.1	75.5	75.5	71.8	71.8	82.7
3′	78.1	78.6	78.6	72.8	72.8	73.2
4′	71.3	71.1	71.1	74.0	73.9	77.3
5′	67.1	67.3	67.3	72.3	72.2	76.1
6′				18.3	18.3	171.1
1″						101.4
2″						76.0
3″						77.6
4″						71.2
5″						78.3
6″						62.4
1‴						105.2
2‴						71.8
3‴						72.8
4‴						74.0
5‴						72.3
6‴						18.3

δ_C 38.4 (C-1), 142.0 (C-5), 51.7 (C-9), and 37.9 (C-10), and the H_2-4/C-5 and C-6 HMBC correlations placed a first trisubstituted double bond at C-5 (Fig. 2). The key H-20, H_3-21/C-22, and H_3-24,[1] H-25/C-23 HMBC correlations placed the disubstituted double bond at $\Delta^{22,23}$ of

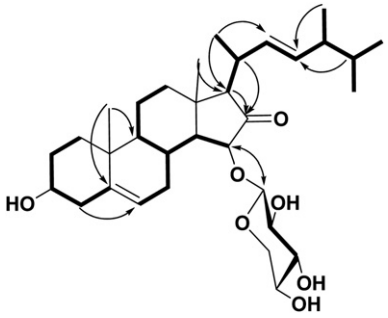

Fig. 2. Key HMBC (H→C) and COSY (bold line) correlations for **1**.

the side chain, whereas the HMBC correlations of the protons at δ_H 2.02 (H-17) and 2.53 (H-20) with the carbon at δ_C 218.9 placed the ketone at C-16. The resulting two oxygenated methines were placed at C-3 and C-15 due to ^{1}H–^{1}H COSY correlations (Fig. 2).

On the other hand, a unique sugar residue was evidenced in the HSQC spectrum of **1** by the characteristic signals of an anomeric proton at δ_H 4.77 (d, J=7.8 Hz) and δ_C 103.5. MS–MS fragmentation evidenced the loss of m/z 132 corresponding to a cyclic pentose. Analysis of the COSY spectrum allowed the assignment of the C-1′/C-2′/C-3′/C-4′/C-5′spin system. The deshielded AMX spin system in the ^{1}H NMR spectrum at δ_H 3.18 (t, J=10.9 Hz), 3.85 (dd, J=11.5, 5.5 Hz), and 3.48 (m) confirmed the presence of a pentopyranose, which was further identified as a xylose by interpretation of the coupling constant values of H-2′ (dd, J=8.9, 7.8 Hz) and H-3′ (t, J=9.0 Hz).[13] This sugar residue was linked to the aglycone at C-15 because of the key H-1′/C-15 and H-15/C-1′ HMBC correlations. The large coupling constant value for the doublet assigned to H-1′ (J=7.8 Hz) implied that the xylose was connected to the aglycone through a β-glycosidic linkage. The D absolute configuration of xylose was obtained by chiral GC analysis of the acetylated sugar residue after acid methanolysis of **1**.[14]

The relative configuration of the aglycone part of **1** was assigned on the basis of NOESY NMR data interpretation as well as coupling constant values. First, the hydrogen at H-3 was placed on the α face of the skeleton due to the vicinal coupling constant values of J=10.9 and 4.5 Hz (δ_H 3.41, tt) (Fig. 3). The key H-7α/H-9/H-14 NOE correlations strongly suggested that all these protons were placed on the same α side of the molecule. Configuration at C-15 was deduced from the absence of a H_3-18/H-15 NOE correlation, present in synthetic compounds with the same D ring and a H-15 on the β face of the steroid.[15] In addition, the constant value of J=7.3 Hz between H-15 and H-14 was consistent with an α orientation of H-15, whereas values of 11.5 or 13.5 Hz were observed in the case of

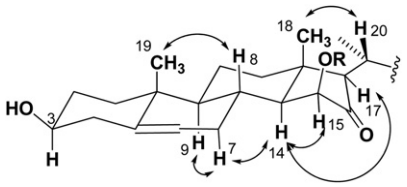

Fig. 3. Key NOESY correlations for the aglycone of **1**.

a β orientation for this hydrogen.[15–17] Because no strong H-17/H$_3$-18 NOE correlation was distinguishable we assumed the natural α orientation for H-17, which was also supported by a small H-14/H-17 NOE correlation.[18,19] The unusual coupling constant value of 5.5 Hz between H-17 and H-20 was nevertheless questioning. However, the α position for H-17 was further supported by its ^{13}C chemical shift at δ_C 69.0 ppm and comparison with literature data. During the oxidation of some steroids hydroxylated at C-16, an epimerization at C-17 was observed with a C-16 keto steroid. For the H-17β configuration the authors reported δ_C 60.7 ppm, whereas a strong deshielding at δ_C 70.9 ppm was observed for the H-17α epimer, very close to our value.[20] The coupling constant between H-22 and H-23 (J=15.4 Hz) was consistent with an *E* configuration for the disubstituted double bond. Comparison of the chemical shifts of the hydrogen side chains with published data allowed the assignment of the configurations at C-20 (*R*) and C-24 (*R*) as an usual ergostane.[21,22]

The negative Cotton effects at 325 nm ($\Delta\varepsilon$ −0.32) in the CD spectrum of **1** were assigned to the $n\rightarrow\pi^*$ transition of the ketone at C-16. A conformational analysis was performed on the usual stereoisomer using the Density Functional Theory (DFT) method at B3LYP/6-31+G(d) level, which gave 12 conformers of relative energies below 5 kcal mol^{-1}. The calculation was run on the 4 lowest energy DFT structures, which represent more than 80% of the population. A very good agreement was observed between the experimental CD spectrum of **1** and the TDDFT calculated spectrum of **1** with this stereochemistry (Fig. 4), which allowed us to propose the depicted relative and absolute configurations for the aglycone part of **1** (Fig. 1). Performing the same theoretical CD spectra with all the four stereoisomers at C-15 and C-17, observation was made that the position of the oxygen at C-15 was critical for the sign of the Cotton effect. Placing the oxygen in the β face induced a negative Cotton effect for both epimers at C-17. On this basis, the structure of compound **1** was established as (*E*)-3β-hydroxy-15β-*O*-(β-D-xylopyranosyl)ergosta-5,22-dien-16-one.

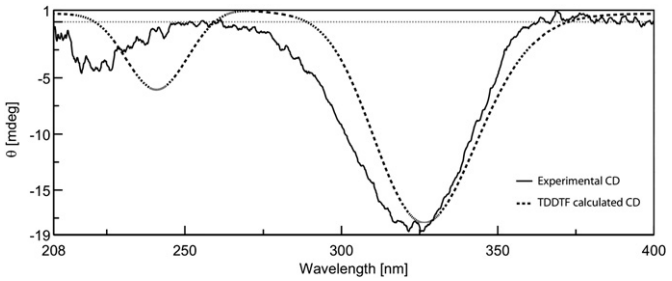

Fig. 4. Experimental and calculated CD spectra of **1**.

The molecular formula of **2** was established as $C_{33}H_{54}O_7$ by HRESIMS (m/z 585.3765 [M+Na]$^+$), which showed the presence of two additional protons in comparison to **1**. The ^{1}H and ^{13}C NMR data were similar to those of **1**, which indicated the occurrence of a similar steroidal skeleton and sugar residue. Differences were located on the D ring where the lack of the signal at δ_C 218.9 (C-16) and the appearance of two signals at δ_C 74.6/δ_H 4.26 suggested the replacement of the carbonyl by a hydroxyl group at C-16. The assignment of the C-14/C-15/C-16/C-17/C-20 spin system by the COSY spectrum confirmed this assumption. We assumed that the stereochemistry was the same as for compound **4** where the signals were fully resolved and all four H-14, H-15, H-16, and H-17 hydrogens placed on the α side of the molecule. Indeed, chemical shifts and coupling constants of H-15 and H-16 were found to be very similar for both products. On this basis, the structure of compound **2** was established as (*E*)-15β-*O*-(β-D-xylopyranosyl) ergosta-5,22-diene-3β,16β-diol.

The molecular formula of compound **3** was determined as $C_{32}H_{52}O_7$ by HRESIMS (m/z 571.3613 [M+Na]$^+$), which involved the loss of a methylene unit comparing to **2**. Differences in their ^{1}H NMR spectra were easily located on the aglycone side chain, where the lack of the characteristic signal at δ_H 0.95 (d, J=6.6 Hz, H$_3$-24^1) suggested that a methyl was absent at C-24. The presence of a new methylene at δ_H 1.90 and 1.86 and δ_C 43.4 was also consistent with this assumption. In consequence, the structure of **3** was deduced to be (*E*)-15β-*O*-(β-D-xylopyranosyl)cholesta-5,22-diene-3β,16β-diol.

The molecular formula of **4** was assigned as $C_{35}H_{62}O_8$ by HRESIMS (m/z 633.4341 [M+Na]$^+$). The ^{13}C and ^{1}H NMR spectra of **4** evidenced that no double bond was present in the structure. Comparing with the spectral data of acanthifoliosides A–C (**1**–**3**), significant changes were observed for the aglycone and sugar residue of **4**. The ^{13}C NMR spectrum of **4** displayed 35 carbon signals, 29 corresponding to the aglycone part and six to the glycoside. The ^{1}H NMR spectrum exhibited the characteristic steroid signals: two methyl groups on quaternary carbons at δ_H 0.87 (s, H$_3$-19) and 1.05 (s, H$_3$-18), three methyl groups on tertiary carbons at δ_H 0.90 (d, J=6.8 Hz, H$_3$-26), 0.96 (d, J=6.8 Hz, H$_3$-27), and 1.01 (d, J=6.6 Hz, H$_3$-21), and one methyl group on a secondary carbon at δ_H 0.97 (t, J=7.1 Hz, H$_3$-24^2). All these data were consistent with a poriferastane/stigmastane skeleton. The analysis of HSQC correlations clearly showed the occurrence of five secondary oxygenated carbons (δ_C 63.9, 71.2, 71.9, 70.0, and 86.2), that were placed at C-17, C-15, C-3, C-23, and C-16 by a combination of COSY and HMBC spectra interpretation. Moreover, the sugar portion of compound **4** showed in the ^{1}H NMR spectrum a new methyl signal at δ_H 1.30 (d, J=6.2 Hz, H$_3$-6′), which suggested the presence of a deoxysugar. The interpretation of coupling constants of the corresponding ^{1}H NMR signals led us to propose a rhamnopyranose unit.[13] Chiral GC analysis allowed us to identify the usual L absolute configuration of this sugar.[23] The H-1′ anomeric proton exhibited a signal at δ_H 4.77 (d, J=3.2 Hz), indicating that the glycoside and the aglycone were connected through an α-glycosidic linkage. Finally, the sugar was linked to the aglycone at C-16 due to the key H-1′/C-16 HMBC correlation. Confirmation was made by the strong deshielding of C-16 from 74 ppm for compounds **2** and **3** to 86 ppm for **4**.

The relative stereochemistry of **4** was established by interpretation of coupling constant values and NOESY data, because in this case no overlapping occurred for all the ^{1}H signals of the D ring. NOESY cross-peaks between H-14/H-15/H-16/H-17 led us to assume that all these protons were placed on the same α face. Because such configurations were already observed for saponins isolated from starfishes we decided to confirm this result comparing the coupling constants for H-15 and H-16. Values around 2.0 Hz are consistent with a trans configuration between both hydroxyls on the cyclopentane D ring.[15,24] Because we measured a coupling constant of 6.2 Hz between these two hydrogens, the relative configuration was cis. After comparison with literature data and modeling with Chem3D (MM2) and MestreJ,[25] using the HLA empirical generalization of the Karplus equation,[26] the only possibility was an all cis relative configuration for the D ring substituents.[27–29] Determination of the configuration of the side chain was rendered difficult because the low quantity of material did not allow us to perform the Mosher method. To the best of our knowledge, there is no natural steroid with a similar side chain,

which prevented any NMR data comparison. There are relatively few examples of such a side chain in the literature and comparison between chemical shifts was highly uncertain.[30,31] Nevertheless, two stereochemical studies of closely related 23-deoxybrassinosteroids allowed us to strongly suggest a trans configuration for compounds **4**–**6**. NMR investigations and molecular modeling of a C-23/C-24 *syn* configuration did not evidence the same NOE correlations,[32] while the H-23 signal at δ_H 3.70 ppm (ddd, J=10.5, 4.8, 1.9 Hz) for 22-deoxy-24-epiteasterone characterized by a trans configuration exhibited very similar coupling constant values.[33] Confirmation of both configurations at C-23 and C-24 would nevertheless require deeper stereochemical analyses. Compound **4** was established as 16β-*O*-(α-L-rhamnopyranosyl)-5α-poriferastane-3β,15β,23*S*-triol.

Compound **5** exhibited the molecular formula $C_{35}H_{60}O_8$ as indicated by HRESIMS (m/z 631.4180 $[M+Na]^+$), which involved the presence of an additional unsaturation comparing to **4**. Both compounds exhibited very similar NMR spectra and they were proven to share the same side chain and sugar residue. The structural difference lied in the presence of a double bond at C-5/C-6 due to the signals at δ_H 5.38 (H-6)/δ_C 122.5 (C-6) and δ_C 142.1 (C-5) as previously described for acanthifoliosides A–C (**1**–**3**). Thus, **5** was deduced to be 16β-*O*-(α-L-rhamnopyranosyl)poriferast-5-ene-3β,15β,23*S*-triol.

The molecular formula of acanthifolioside F (**6**) ($C_{47}H_{80}O_{19}$) was calculated from the HRESIMS spectrum (m/z 971.5198 $[M+Na]^+$). Comparison between the NMR spectra of **6** and those of acanthifoliosides D and E (**4** and **5**) did not evidence any strong difference between their steroid parts. Changes were mostly observed in the NMR spectra of the sugar part, where for the first time three anomeric protons were evidenced in the ^{1}H NMR spectrum. An α-rhamnopyranose was identified by comparison with previous data of compounds **4** and **5**. A β-glucopyranose and a β-glucuronic acid were identified by comparison with previous data obtained for pandarosides. The sugar identification was completed by chiral GC analysis, which allowed us to assign the absolute configuration of the sugar residues as D-GluUA, D-Glu, and L-Rha. Finally, interpretation of ^{13}C deshieldings on the glucuronic acid residue in addition to H-1‴/C-4′ and H-1″/C-2′ HMBC correlations allowed us to identify the sequence of the trisaccharide unit as (β-D-glucopyranosyl-(1→2))-(α-L-rhamnopyranosyl-(1→4))-β-D-glucuronic acid, the GlcUA residue being attached to the aglycon at C-16 due to H-1′/C-16 HMBC cross-peaks.

The ion at m/z 985.5386 $[M+Na]^+$ in the HRESIMS established the molecular formula of compound **7** as $C_{48}H_{82}O_{19}$, which indicated the presence of an additional methylene unit in comparison with **6**. The ^{1}H and ^{13}C NMR data were very similar to those of **6** except for the new signals at δ_H 3.76 (s, H_3–CO) and δ_C 52.8 (O–CH_3), which suggested the presence of a methoxyl group. The H_3–CO/C-6′ HMBC correlation allowed us to identify the methyl ester of acanthifolioside F (**6**). This compound could be formed during the extraction process as previously observed for pandarosides.

All acanthifoliosides share a common 15,16 dioxidized D ring with one sugar residue at C-15 or C-16. They consequently differ from the previously isolated pandarosides characterized by a 15,16 diketone enolized at C-16. Mostly found in starfishes, some analogs have been recognized as cytotoxins.[15]

From a taxonomic point of view, the large amount of steroidal saponins was unexpected in this sponge as they are mainly found in *Asteropus*, *Melophlus*, and *Erylus* genera. Even if the genus *Pandaros* belongs to the Poecilosclerida order, a recent phylogenetic study by Erpenbeck put apart the genera *Pandaros* and *Ectyoplasia* from the other Poecilosclerida sponges, known to produce a large variety of complex alkaloids.[34] They seem to be much more closely related to Asterophorida sponges, a rich source of saponins. Some saponins were already described from *Ectyoplasia ferox* and our study underlined a high amount of steroidal saponins in *P. acanthifolium*.[35,36] All these chemotaxonomic considerations are fully consistent with the result of Erpenbeck.

Antiprotozoal bioassays were performed on compounds **1**–**7**. Even if moderate activities were detected on *L. donovani* and *P. falciparum* acanthifoliosides appear less potent than pandarosides (Table 3).

Table 3
In vitro antiprotozoal and cytotoxic activities of sponge-derived compounds **1**–**7**. IC_{50} values are in μM

	T. b. rhodesiense	*T. cruzi*	*L. donovani*	*P. falciparum*	Cytotoxicity L6 cells
1	94.8	27.6	20.7	21.6	25.9
2	32.0	28.6	8.5	7.6	42.3
3	32.3	30.6	7.5	8.8	31.9
4	30.8	15.3	5.7	15.0	7.0
5	27.4	10.6	9.4	12.9	8.5
6	24.8	77.4	29.0	37.0	89.9
7	6.4	22.2	5.7	9.2	18.3
Stds	0.010[a]	2.64[b]	0.51[c]	0.20[d]	0.012[e]

Standard compounds:
[a] Melarsoprol.
[b] Benznidazole.
[c] Miltefosine.
[d] Chloroquine.
[e] Podophyllotoxin.

3. Experimental section

3.1. General experimental procedures

Optical rotations were measured on Perkin–Elmer 343 polarimeter equipped with a 10-cm microcell. CD spectrum of **1** was measured using a JASCO J-810 spectropolarimeter. IR spectra were obtained with a Perkin–Elmer Paragon 1000 FT-IR spectrometer. UV measurements were performed on a Varian Cary 300 Scan UV–visible spectrometer. Electrospray ionization (ESI) mass spectra were obtained with a Bruker Esquire 3000 Plus spectrometer in the positive or negative mode. High-resolution mass spectra (HRESIMS) were obtained from a LTQ Orbitrap mass spectrometer (Thermo Finnigan). NMR experiments were performed on a Bruker Avance 500 MHz spectrometer. Chemical shifts (δ in ppm) are referenced to the carbon (δ_C 49.0) and residual proton (δ_H 3.31) signals of CD_3OD, the solvent with multiplicity (s singlet, d doublet, t triplet, m multiplet). Flash Chromatography fractionation was performed on an Armen Spot Flash instrument equipped with a UV detector. Column chromatography was performed using DIOL as the stationary phase (40–63 μm, Merk KGaA 64271 Darmstadt, Germany). HPLC separation and purification were carried out on a Waters 600 system equipped with a Waters 996 Photodiode Array detector coupled with a Sedex 55 ELSD (SEDERE, France), and a Waters 717 plus Autosampler. TLC was performed with Kieselgel 60 F_{254} (Merck glass support plates) and spots were detected after spraying with 10% H_2SO_4 in EtOH reagent and heating.

3.2. Biological material

The marine sponge was collected off Martinique Island in summer 2003 by SCUBA diving (Canyons de Babodie 14°45,982 N, 61°11,902 W). A voucher specimen (ORMA8362) identified by Dr. Jean Vacelet, has been deposited in the Center d'Océanologie de Marseille (Endoume, France). The sponge was kept frozen from collection until the extraction process.

3.3. Extraction and isolation

The frozen sponge (536 g) was cut into pieces of about 1 cm^3 and extracted with MeOH/CH_2Cl_2 1:1 at room temperature yielding

20.0 g of crude extract after solvent evaporation. The crude extract was fractionated by RP-C_{18} flash chromatography (elution with a decreasing polarity gradient of H_2O/MeOH from 1:0 to 0:1, then MeOH/CH_2Cl_2 from 1:0 to 0:1). The MeOH 100% (1.1 g) fraction was then subjected to DIOL column chromatography (elution with an increasing polarity gradient of CH_2Cl_2/MeOH from 95:5 to 0:100), this separation step yielded seven fractions after the TLC analysis (see details in Supplementary data). The aliquots corresponding to MeOH (5–15%, 40 mg) were then subjected to RP-C_{18} semi-preparative HPLC (Phenomenex, Luna C_{18}, 250×10 mm, 5 μm) with an isocratic mobile phase of H_2O/MeOH/TFA (flow 3.0 ml min^{-1}, 10:90:0.1) to yield pure compounds **3** and **2** (t_R: 19.1 and 23.3 min; 3.7 and 3.3 mg, respectively); whereas the subfraction (14.0–16.0 min; 11.2 mg) was further chromatographied in analytic HPLC (Phenomenex, Gemini C_6-phenyl, 250×3 mm, 5 μm) with an isocratic mobile phase of H_2O/CH_3CN/TFA (flow 0.5 ml min^{-1}, 50:50:0.1) to afford pure metabolites **5**, **4**, and **1** (t_R: 13.2, 14.8, and 21.1 min; 1.0, 1.7, and 1.2 mg, respectively). On the other hand, the H_2O/MeOH 1:3 (220 mg) fraction, which had been obtained from RP-C_{18} flash chromatography, was then subjected to RP-C_{18} semi-preparative HPLC (Phenomenex, Luna C_{18}, 250×10 mm, 5 μm) with a gradient of H_2O/MeOH/TFA (flow 3.0 ml min^{-1} from 28:72:0.1 to 20:80:0.1) to obtain a complex chemical profile (see Supplementary data). A subsequent mixture (33.0–34.0 min; 10.0 mg) was finally purified by analytical HPLC (C_6-phenyl) with a gradient of H_2O/CH_3CN/formic acid (flow 0.5 ml min^{-1}, 62:38:0.1) to afford pure compounds **6** and **7** (t_R: 15.8 and 24.3 min; 2.0 and 1.6 mg, respectively).

3.4. Computational method

Quantum chemical calculations were performed on the four diastereoisomers at C-15 and C-17 of compound **1**. The Gaussian03W package[37] has been used for the conformational search as well as for circular dichroism calculations. Density functional theory (DFT) with B3LYP functional[38] and Pople's 6.31+G(d) basis set[39] was used on the lowest energy conformer. TDDFT was employed to calculate excitation energy (in eV) and rotatory strength R in dipole velocity (R_{vel}) and dipole length (R_{len}) forms. The Boltzmann weighted rotatory strengths were simulated in ECD curve by using a corrected Gaussian function.

$$\Delta\varepsilon(E) = \frac{1}{2.296\times10^{-39}\sqrt{2\pi}\Delta}\sum_{a}\Delta E_{0a}R_{0a}e^{-\left(\frac{(E-\Delta E_{0a})}{2\Delta}\right)^2}$$

where Δ is half the width of the band at $\frac{1}{e}$ peak height expressed in energy units. The parameters ΔE_{0a} and R_{0a} are the excitation energies and the rotatory strengths for transition from 0 to a, respectively, Δ=0.1 eV and R_{vel} were used.

3.5. Acanthifolioside A (1)

(*E*)-3β-Hydroxy-15β-*O*-(β-D-xylopyranosyl)-ergosta-5,22-dien-16-one. White amorphous solid; $[\alpha]_D^{20}$ −87.3 (*c* 0.14, MeOH); CD (MeOH, *c* 2.5×10^{-4} M) λ_{max} ($\Delta\varepsilon$) 325 (−0.32) nm. IR (thin film): γ_{max} 3490, 1688 and 1644 cm^{-1}; ^{1}H NMR see Table 1; ^{13}C NMR see Table 2; HRESIMS (+): *m*/*z* 583.3610 $[M+Na]^+$ (calcd for $C_{33}H_{52}NaO_7$, 583.3605, Δ 0.85 ppm).

3.6. Acanthifolioside B (2)

(*E*)-15β-*O*-(β-D-Xylopyranosyl)ergosta-5,22-diene-3β,16β-diol. White amorphous solid; $[\alpha]_D^{20}$ −22.5 (*c* 0.16, MeOH); IR (thin film): γ_{max} 3436 cm^{-1}; ^{1}H NMR see Table 1; ^{13}C NMR see Table 2; HRESIMS (+): *m*/*z* 585.3765 $[M+Na]^+$ (calcd for $C_{33}H_{54}NaO_7$, 585.3762, Δ 0.51 ppm).

3.7. Acanthifolioside C (3)

(*E*)-15β-*O*-(β-D-Xylopyranosyl)cholesta-5,22-diene-3β,16β-diol. White amorphous solid; $[\alpha]_D^{20}$ −25.0 (*c* 0.14, MeOH); IR (thin film): γ_{max} 3422 cm^{-1}; ^{1}H NMR see Table 1; ^{13}C NMR see Table 2; HRESIMS (+): *m*/*z* 571.3613 $[M+Na]^+$ (calcd for $C_{32}H_{52}NaO_7$, 571.3605, Δ 1.4 ppm).

3.8. Acanthifolioside D (4)

16β-*O*-(α-L-Rhamnopyranosyl)-5α-poriferastane-3β,15β,23*S*-triol. White amorphous solid; $[\alpha]_D^{20}$ −15.6 (*c* 0.13, MeOH); IR (thin film): γ_{max} 3420 cm^{-1}; ^{1}H NMR see Table 1; ^{13}C NMR see Table 2; HRESIMS (+): *m*/*z* 633.4341 $[M+Na]^+$ (calcd for $C_{35}H_{62}NaO_8$, 633.4347, Δ −0.95 ppm).

3.9. Acanthifolioside E (5)

16β-*O*-(α-L-Rhamnopyranosyl)poriferast-5-ene-3β,15β,23*S*-triol. White amorphous solid; $[\alpha]_D^{20}$ −30.0 (*c* 0.07, MeOH); IR (thin film): γ_{max} 3430 cm^{-1}; ^{1}H NMR see Table 1; ^{13}C NMR see Table 2; HRESIMS (+): *m*/*z* 631.4180 $[M+Na]^+$ (calcd for $C_{35}H_{60}NaO_8$, 631.4171, Δ 1.43 ppm).

3.10. Acanthifolioside F (6)

16β-*O*-[β-D-Glucopyranosyl-(1→2)-α-L-rhamnopyranosyl-(1→4)-β-D-glucopyranosyloxyuronic acid]-5α-poriferastane-3β,15β,23*S*-triol. White amorphous solid; $[\alpha]_D^{20}$ −20.7 (*c* 0.15, MeOH); IR (thin film): γ_{max} 3420 cm^{-1}; ^{1}H NMR see Table 1; HRESIMS (+): *m*/*z* 971.5198 $[M+Na]^+$ (calcd for $C_{47}H_{80}NaO_{19}$, 971.5186, Δ 1.24 ppm).

3.11. Methyl ester of acanthifolioside F (7)

White amorphous solid; $[\alpha]_D^{20}$ −19.2 (*c* 0.13, MeOH); ^{1}H NMR (500 MHz, CD_3OD) for the uronic residue: δ 4.60 (d, *J*=7.6 Hz, H-1′), 3.43 (t, *J*=7.5 Hz, H-2′), 3.56 (m, H-3′, and H-4′), 3.81 (d, *J*=9.5 Hz, H-5′), 3.76 (s, CH_3O–); ^{13}C NMR (125 MHz, CD_3OD) for the uronic residue: δ 101.8 (C-1′), 82.7 (C-2′), 73.0 (C-3′), 77.0 (C-4′), 76.5 (C-5′), 171.1 (C-6′), 52.8 (CH_3O–); HRESIMS (+): *m*/*z* 985.5386 $[M+Na]^+$ (calcd for $C_{48}H_{82}NaO_{19}$, 985.5421, Δ −3.55 ppm).

3.11.1. Methanolysis of acanthifoliosides. Compounds **2**, **4**, and **6** (0.30 mg) were dissolved in a HCl (7 N, 1.0 ml)–MeOH solution (Supelco, USA) and heated at 75 °C for 4 h. The reaction mixture was neutralized with $NaHCO_3$, evaporated to dryness, and then partitioned between $CHCl_3$ and H_2O. The H_2O layer was dried under reduced pressure to afford a mixture of methyl glycosides.

3.11.2. Derivatization of the hydrolyzate for GC analysis. The methanolysis products were dissolved in a mixture of dry CH_2Cl_2/pyridine (1:1) and an excess of acetic anhydride was added. The reaction was stirred at 25 °C for 8 h. The mixture was then dried and dissolved in AcOEt for GC analysis.

3.11.3. Chiral GC analysis. GC analysis was carried out on a Chirasil-L-Val Alltech capillary column (25 m×0.25 mm, i.d.), using a Hewlett Packard Mass Selective Detector 5972 series. A temperature gradient system was used for the oven, starting at 100 °C for 3 min and increasing up to 200 °C at a rate of 10 °C/min. Peaks of the hydrolyzate of pandarosides and sugar standards were detected at 15.3 min (D-glc), 13.2 min (D-xyl), 12.1 min (D-glcUA), and 11.5 min (L-rha). Because some retention times fluctuated, the identity of the

enantiomers was confirmed by injection of a mixture of the sample and standards acetylated using the same protocol.

3.12. Antiprotozoal assays

Antimalarial activity against *P. falciparum*. In vitro parasite growth inhibition was assessed by a modified of [^{3}H]-hypoxanthine incorporation assay using the chloroquine- and pyrimethamine-resistant K1 strain and the standard drug chloroquine. Briefly, compounds were dissolved in 100% DMSO and twofold dilution series of the compounds prepared in assay medium (RPMI 1640 supplemented with 5% Albumax II, 0.2% w/v glucose, 0.03% L-glutamine) were added to each well of microtiter plates. Parasite cultures (50 μl) were added to each well reaching a final volume of 100 μl per well (final DMSO concentration ≤0.25%). Plates were incubated at 37 °C for 48 h and 0.1 μCi ^{3}H-hypoxanthine (Perkin–Elmer, Hounslow, UK) was added to each well. The plates were mixed and incubated for another 24 h. The experiment was terminated by placing the plates in a −80 °C freezer. Plates were thawed and harvested onto glass fiber filter mats using a 96-well cell harvester (Harvester 96, Tomtec, Oxon, UK). The incorporated radioactivity was counted using a liquid BetaLux scintillation counter (Wallac). Data acquired by the Wallac BetaLux scintillation counter were exported into a Microsoft® Excel spreadsheet (Microsoft), and the IC_{50} values of each compound were calculated.

Trypanocidal activity against *T. b. rhodesiense*. The STIB 900 strain parasite and the standard drug, melarsoprol, were used for the assay. Minimum Essential Medium (50 μl) supplemented with 25 mM HEPES, 1 g/l additional glucose, 1% MEM non-essential amino acids (100×), 0.2 mM 2-mercaptoethanol, 1 mM Na-pyruvate, and 15% heat-inactivated horse serum was added to each well of a 96-well microtiter plate.[40,41] Serial drug dilutions of seven threefold dilution steps covering a range from 90 to 0.123 μg/ml were prepared. Then 10^4 bloodstream forms of *T. b. rhodesiense* STIB 900 in 50 μl was added to each well and the plate incubated at 37 °C under a 5% CO_2 atmosphere for 72 h. Resazurin solution (10 μl, 12.5 mg resazurin dissolved in 100 ml double-distilled water) was then added to each well and incubation continued for a further 2–4 h.[42] Then the plates were read in a Spectramax Gemini XS microplate fluorometer (Molecular Devices Cooperation, Sunnyvale, CA, USA) using an excitation wavelength of 536 nm and an emission wavelength of 588 nm. Data were analyzed using the microplate reader software Softmax Pro (Molecular Devices Cooperation, Sunnyvale, CA, USA).

Trypanocidal activity against *T. cruzi*. Rat skeletal myoblasts (L6 cells) were seeded in 96-well microtitre plates at 2000 cells/well in 100 μl RPMI 1640 medium with 10% FBS and 2 mM L-glutamine. After 24 h the medium was removed and replaced by 100 μl per well containing 5000 trypomastigote forms of *T. cruzi* Tulahuen strain C2C4 containing the β-galactosidase (Lac Z) gene.[43] After 48 h, the medium was removed from the wells and replaced by 100 μl fresh medium with or without a serial drug dilution of seven threefold dilution steps covering a range from 90 to 0.123 μg/ml. After 96 h of incubation the plates were inspected under an inverted microscope to assure growth of the controls and sterility. Then the substrate CPRG/Nonidet (50 μl) was added to all wells. A color reaction developed within 2–6 h and read photometrically at 540 nm. Data were transferred into the graphic programme Softmax Pro (Molecular Devices), which calculated IC_{50} values.

Leishmanicidal activity against *L. donovani*. Amastigotes of *L. donovani* strain MHOM/ET/67/L82 were grown in axenic culture at 37 °C in SM medium at pH 5.4 supplemented with 10% heat-inactivated fetal bovine serum under an atmosphere of 5% CO_2 in air. Culture medium (100 μl) with 10^5 amastigotes from axenic culture with or without a serial drug dilution was seeded in 96-well microtitre plates. Serial drug dilutions covering a range from 90 to 0.123 μg/ml were prepared. After 72 h of incubation the plates were inspected under an inverted microscope to assure growth of the controls and sterile conditions. 10 μl of a resazurin solution was then added to each well and the plates incubated for another 2 h.[44] Then the plates were read in a Spectramax Gemini XS microplate fluorometer using an excitation wavelength of 536 nm and an emission wavelength of 588 nm. Data were analyzed using the software Softmax Pro. Decrease of fluorescence (=inhibition) was expressed as percentage of the fluorescence of control cultures and plotted against the drug concentrations. From the sigmoidal inhibition curves the IC_{50} values were calculated.

3.13. Cytotoxicity against L6 cells

Assays were performed in 96-well microtitre plates, each well containing 100 μl of RPMI 1640 medium supplemented with 1% L-glutamine (200 mM) and 10% fetal bovine serum, and 4×10^4 L6 cells. Serial drug dilutions of seven threefold dilution steps covering a range from 90 to 0.123 μg/ml were prepared. After 72 h of incubation the plates were inspected under an inverted microscope to assure growth of the controls and sterile conditions. Alamar Blue (10 μl, 12.5 mg resazurin dissolved in 100 ml double-distilled water) was then added to each well and the plates were incubated for another 2 h. Then the plates were read with a Spectramax Gemini XS microplate fluorometer using an excitation wavelength of 536 nm and an emission wavelength of 588 nm. Data were analyzed using the microplate reader software Softmax Pro. Podophyllotoxin was the standard drug used.

Acknowledgements

We are grateful to UNESCO and Boehringer Ingelheim Fonds for financial support provided by two fellowships (E.L.R) and also to PharmaMar (Madrid). We thank J. Vacelet (Centre d'Océanologie de Marseille) for careful taxonomical sponge identification, M. Gaysinski and the PFTC of Nice for assistance in recording the NMR spectroscopic experiments, J.-M. Guigonis for assistance in recording the HRMS experiments, and Abimael D. Rodríguez for assistance in GC analyses. We finally thank Mr. le préfet de la Martinique and the DIREN for their help in the collection of Caribbean marine invertebrates.

Supplementary data

Separation and purification details including HPLC profiles, ^{1}H, ^{13}C, 2D NMR spectra for compounds **1**–**7**, experimental and calculated CD spectra of **1**. Supplementary data associated with this article can be found online version at doi:10.1016/j.tet.2010.11.103. These data include MOL files and InChIKeys of the most important compounds described in this article.

References and notes

1. Iorizzi, M.; De Marino, S.; Zollo, F. *Curr. Org. Chem.* **2001**, *5*, 951–973.
2. Espada, A.; Jimenez, C.; Rodriguez, J.; Crews, P.; Riguera, R. *Tetrahedron* **1992**, *48*, 8685–8696.
3. Ksebati, M. B.; Schmitz, F. J.; Gunasekera, S. P. *J. Org. Chem.* **1988**, *53*, 3917–3921.
4. Schmitz, F. J.; Ksebati, M. B.; Gunasekera, S. P.; Agarwal, S. *J. Org. Chem.* **1988**, *53*, 5941–5947.
5. Dai, H.-F.; Edrada, R. A.; Ebel, R.; Nimtz, M.; Wray, V.; Proksch, P. *J. Nat. Prod.* **2005**, *68*, 1231–1237.
6. Lee, H.-S.; Seo, Y.; Cho, K. W.; Rho, J.-R.; Shin, J.; Paul, V. J. *J. Nat. Prod.* **2000**, *63*, 915–919.
7. Fouad, M.; Al-Trabeen, K.; Badran, M.; Wray, V.; Edrada, R.; Proksch, P.; Ebel, R. *ARKIVOC* **2004**, 17–27 (Gainesville, FL, U.S.).
8. Shin, J.; Lee, H.-S.; Woo, L.; Rho, J.-R.; Seo, Y.; Cho, K. W.; Sim, C. J. *J. Nat. Prod.* **2001**, *64*, 767–771.
9. Takada, K.; Nakao, Y.; Matsunaga, S.; van, S. R. W. M.; Fusetani, N. *J. Nat. Prod.* **2002**, *65*, 411–413.

10. Cachet, N.; Regalado, E. L.; Genta-Jouve, G.; Mehiri, M.; Amade, P.; Thomas, O. P. *Steroids* **2009**, *74*, 746–750.
11. Regalado, E. L.; Tasdemir, D.; Kaiser, M.; Cachet, N.; Amade, P.; Thomas, O. P. *J. Nat. Prod.* **2010**, *73*, 1404–1410.
12. Schmitz, F. J.; Prasad, R. S.; Gopichand, Y.; Hossain, M. B.; Van der Helm, D.; Schmidt, P. *J. Am. Chem. Soc.* **1981**, *103*, 2467–2469.
13. Agrawal, P. K. *Phytochemistry* **1992**, *31*, 3307–3330.
14. König, W. A.; Benecke, I.; Bretting, H. *Angew. Chem., Int. Ed.* **1981**, *20*, 693–694.
15. Izzo, I.; de Riccardis, F.; Sodano, G. *J. Org. Chem.* **1998**, *63*, 4438–4443.
16. Riccio, R.; Minale, L.; Pagonis, S.; Pizza, C.; Zollo, F.; Pusset, J. *Tetrahedron* **1982**, *38*, 3615–3622.
17. Minale, L.; Pizza, C.; Zollo, F.; Riccio, R. *Tetrahedron Lett.* **1982**, *23*, 1841–1844.
18. Ono, M.; Shiono, Y.; Yanai, Y.; Fujiwara, Y.; Ikeda, T.; Nohara, T. *Chem. Pharm. Bull.* **2008**, *56*, 1499–1501.
19. Zhang, L.; Liu, J.-Y.; Xu, L.-Z.; Yang, S.-L. *Chem. Pharm. Bull.* **2009**, *57*, 1126–1128.
20. Morzycki, J. W.; Pérez-Díaz, J. O. H.; Santillan, R.; Wojtkielewicz, A. *Steroids* **2010**, *75*, 70–76.
21. Chang, C.-H.; Wen, Z.-H.; Wang, S.-K.; Duh, C.-Y. *Steroids* **2008**, *73*, 562–567.
22. Hua, Z.; Carcache, D. A.; Tian, Y.; Li, Y.-M.; Danishefsky, S. J. *J. Org. Chem.* **2005**, *70*, 9849–9856.
23. Guo, S.; Kenne, L. *Phytochemistry* **2000**, *54*, 615–623.
24. Kicha, A. A.; Ivanchina, N. V.; Kalinovsky, A. I.; Dmitrenok, P. S.; Stonik, V. A. *Steroids* **2009**, *74*, 238–244.
25. Navarro-Vazquez, A.; Cobas, J. C.; Sardina, F. J.; Casanueva, J.; Diez, E. *J. Chem. Inf. Comput. Sci.* **2004**, *44*, 1680–1685.
26. Haasnoot, C. A. G.; De Leeuw, F. A. A. M.; Altona, C. *Tetrahedron* **1980**, *36*, 2783–2792.
27. Kicha, A. A.; Kapustina, I. I.; Ivanchina, N. V.; Kalinovsky, A. I.; Dmitrenok, P. S.; Stonik, V. A.; Pal'yanova, N. V.; Pankova, T. M.; Starostina, M. V. *Russ. J. Bioorg. Chem.* **2008**, *34*, 118–124.
28. Levina, E. V.; Kalinovsky, A. I.; Levin, V. S. *Russ. J. Bioorg. Chem.* **2006**, *32*, 84–88.
29. Wang, W.; Hong, J.; Lee, C.-O.; Im, K. S.; Choi, J. S.; Jung, J. H. *J. Nat. Prod.* **2004**, *67*, 584–591.
30. Giner, J. L.; Margot, C.; Djerassi, C. *J. Org. Chem.* **1989**, *54*, 369–373.
31. Nakane, M.; Morisaki, M.; Ikekawa, N. *Tetrahedron* **1975**, *31*, 2755–2760.
32. Drosihn, S.; Porzel, A.; Brandt, W. *J. Mol. Model.* **2001**, *7*, 34–42.
33. Voigt, B.; Porzel, A.; Bruhn, C.; Wagner, C.; Merzweiler, K.; Adam, G. *Tetrahedron* **1997**, *53*, 17039–17054.
34. Erpenbeck, D.; Van Soest, R. W. M. *Biochem. Syst. Ecol.* **2005**, *33*, 585–616.
35. Cafieri, F.; Fattorusso, E.; Taglialatela-Scafati, O. *Eur. J. Org. Chem.* **1999**, 231–238.
36. Campagnuolo, C.; Fattorusso, E.; Taglialatela-Scafati, O. *Tetrahedron* **2001**, *57*, 4049–4055.
37. Frisch, M.J.; Trucks, G.W.; Schlegel, H.B.; Scuseria, G.E.; Robb, M.A.; Cheeseman, J.R.; Montgomery, J.A., Jr.; Vreven, T.; Kudin, K.N.; C., B.J.; Millam, J.M.; Iyengar, S. S.; Tomasi, J.; Barone, V.; Mennucci, B.; Cossi, M.; Scalmani, G.; Rega, N.; Petersson, G.A.; Nakatsuji, H.; Hada, M.; Ehara, M.; Toyota, K.; Fukuda, R.; Hasegawa, J.; Ishida, M.; Nakajima, T.; Honda, Y.; Kitao, O.; Nakai, H.; Klene, M.; Li, X.; Knox, J.E.; Hratchian, H.P.; Cross, J.B.; Bakken, V.; Adamo, C.; Jaramillo, J.; Gomperts, R.; Stratmann, R.E.; Yazyev, O.; Austin, A.J.; Cammi, R.; Pomelli, C.; Ochterski, J.W.; Ayala, P.Y.; Morokuma, K.; Voth, G.A.; Salvador, P.; Dannenberg, J.J.; Zakrzewski, V.G.; Dapprich, S.; Daniels, A.D.; Strain, M.C.; Farkas, O.; Malick, D.K.; Rabuck, A.D.; Raghavachari, K.; Foresman, J.B.; Ortiz, J.V.; Cui, Q.; Baboul, A.G.; Clifford, S.; Cioslowski, J.; Stefanov, B.B.; Liu, G.; Liashenko, A.; Piskorz, P.; Komaromi, I.; Martin, R.L.; Fox, D.J.; Keith, T.; Al.Laham, M.A.; Peng, C.Y.; Nanayakkara, A.; Challacombe, M.; Gill, P.M.W.; Johnson, B.; Chen, W.; Wong, M. W.; Gonzalez, C.; Pople, J.A. Gaussian, Wallingford, CT, 2004.
38. Lee, C.; Yang, W.; Parr, R. G. *Phys. Rev. B* **1988**, *37*, 785–789.
39. Hariharan, P. C.; Pople, J. A. *Theor. Chim. Acta* **1973**, *28*, 213–222.
40. Baltz, T.; Baltz, D.; Giroud, C.; Crockett, J. *EMBO J.* **1985**, *4*, 1273–1277.
41. Thuita, J. K.; Karanja, S. M.; Wenzler, T.; Mdachi, R. E.; Ngotho, J. M.; Kagira, J. M.; Tidwell, R.; Brun, R. *Acta Trop.* **2008**, *108*, 6–10.
42. Räz, B.; Iten, M.; Grether-Bühler, Y.; Kaminsky, R.; Brun, R. *Acta Trop.* **1997**, *68*, 139–147.
43. Buckner, F. S.; Verlinde, C. L.; La Flamme, A. C.; Van Voorhis, W. C. *Antimicrob. Agents Chemother.* **1996**, *40*, 2592–2597.
44. Mikus, J.; Steverding, D. *Parasitol. Int.* **2000**, *48*, 265–269.